FACILE PREPARATION METHOD FOR MESOPOROUS MFI ZEOLITE BY STEAM ASSISTED TRANSFORMATION OF MONOLITHIC SILICA

Ren-Fu Tsai, Kun-Jia Du, Tzu-Yu Cheng, Grace Hsiuying Ho, Tseng-Chang Tsai*

Department of Applied Chemistry, National University of Kaohsiung, Kaohsiung 811, Taiwan.
*Email: tctsai@nuk.edu.tw

Abstract

Crystallization of monolithic silica by solid state transformation in "steaming" or "boiling" mode for the preparation of mesoporous MFI zeolite is demonstrated. "Steaming" mode is particularly effective for generating mesoporosity in MFI zeolites. The pre-forming pressure of silica monolith affects strongly the crystallinity, morphology and physical property of the MFI zeolite products. The proposed method can prepare wide range of crystal morphology from nm spheres to μm longitudinal rectangles with mesopore size of 5 nm were prepared. The micro/meso porous MFI zeolite shows improved hexane temperature programmed desorption (TPD) capacity at relatively lower TPD temperature than conventional silicalite.

Keywords: steam assisted conversion, dry gel crystallization, monolith silica

Introduction

Zeolites have been widely used in chemical industry. They have low diffusivities of large molecules in the microporous structures. Introducing mesoporosity into zeolites can improve their diffusivities and thus adsorption and catalytic properties[1-5]. Although wide unimodal pore zeolites could have improved diffusivities, the low framework stabilities and discovery of such new zeolites are technical challenges. On the other hand, hierarchical zeolite in the categories of nano-crystalline zeolites [6, 7], zeolite composites and mesoporous zeolites is a viable strategy [8]. Hierarchical zeolite could be prepared by direct synthesis method or post chemical treatments [9-11]. The hierarchical porous structures change with preparation procedures.

Having large inter-crystalline mesopores and external surface area with shortened diffusion length, nano-crystalline zeolites have much improved diffusivity. Nevertheless, the application of nano-crystalline zeolites suffers from some practical problems such as agglomeration of nano-crystals, difficulty of separation and recovery of zeolites.

Zeolite composites are made of highly dispersed or supported zeolite crystals in a matrix material. Self supported zeolite particles in a monolith could form hierarchical porosity to have advantage of high diffusivity, mechanical strength with low pressure drop. Li et al. reported a synthesis method for silicalite monolith by double impregnations with zeolite precursors in the formaldehyde - recercinol aerogel monolith [3]. The silicalite monolith showed excellent catalytic performances for Beckmann rearrangement of cyclohexanone oxime.

Templating synthesis is an effective method for the replication of nano-particles [12] and also for the preparation of mesoporous zeolites [13-19]. The templatesynthesis usually applies the so-called steam assisted conversion (SAC) process [20]. During zeolite synthesis, various porogen generating agents, either hard templates or supramolecules, are embedded inside zeolite crystal by so-called endo-templating or exo-templating method [21]. The reported porogen generating agents include carbon materials [22, 23], anionic surfactants [17],

amphiphilic organosilanes [24], nanosized organic/inorganic particles [25], and poly(methyl methacrylate) nanospheres as a so-called dual functional template for generation of mesoporosity and spherical hierarchically structured zeolites particles [26], etc. Mesopores inside zeolite crystals are generated after removal of porogen materials by combustion or leaching. Tong et al. reported the synthesis of monolithic zeolite Beta with SAC process using carbon as a transitional template [27]. The carbon template was to support the pore channels of the silica monolith beyond collapse during crystallization of the amorphous walls of silica monolith. As a result, the zeolite beta had hierarchical porosity.

By means of SAC process, mesoporous MFI zeolite could be prepared from surfactant containing MCM-41 [4] or from TUD-1 using triethanolamine as meso porogen template [28]. Nevertheless, the templating synthesis route is tedious and material intensive involving preparation of hard or soft template containing silica precursors and removal of templates. This study explores a synthesis method for preparation of mesoporous MFI zeolite directly from monolithic silica by SAC process.

Experimental

Precipitated silica powder was pressed into a monolith at various pressures ranging from 140 to 420 kg/cm^2. Silica powder and monolithic silica were used as raw material. The silica of 0.56 g was impregnated with tetra-propyl ammonium hydroxide (40% TPAOH) solution of 200 μL giving overall composition as SiO_2 :TPA = 1 : 0.06, then was dried at room temperature for 1 day to form TPA-silica composite. Polytetrafluoroethylene (PTFE) lined autoclave was used as crystallizer. With "boiling mode" either by A (acidic solution) or H (neutral water) protocol, the TPA-silica composite was wetted with H_2SO_4 solution (pH = 5) or distilled water of 200 μL, respectively; then was placed at the bottom of a dry autoclave of 25 ml volume. With "steaming" mode by D (dry gel) protocol, the TPA-silica composite was sited on top of a stainless steel grid suspended inside a 182 ml autoclave containing 5 ml distilled water. The TPA-silica composite was subjected to crystallization at 180 ℃ for 12 h. Finally the TPA-silica composite was washed with distilled water and calcined in air at 540 ℃ for 8 h. The sample was denoted as *X*SiPz standing for the conversion of monolithic silica pressurized at z kg/cm^2 with *X* protocol. For example, ASiP280 represents crystallization of monolithic silica pressurized at 280 kg/cm^2 with A protocol at 180 ℃ for 12 h.

All the silica samples including monolithic silica were ground into powder form for characterization. The X-ray diffraction pattern was recorded with a Rigaku Multiflex X-ray Diffractometer using Cu $K\alpha$ radiation at 40 kV and 30 mA. The morphology of zeolite crystal was examined with HITACHI S-3400N scanning electron microscopy (SEM) at 15 kV and 10 mm working distance. Nitrogen adsorption–desorption isotherms and BET surface area measurements were conducted using Micromeritics ASAP2020 at 77 K. The samples of 0.1–0.15 g were first degassed in vacuum at a ramp rate of 10 ℃/min up to 623 K for 8 h. The BET method was used to calculate the specific surface areas. The pore volumes and pore size distributions were derived from the desorption isotherms using the Barrett–Joyner–Halenda (BJH) method. Temperature programmed desorption (TPD) of hexane isomers were conducted in a HP5890 Gas Chromatography equipped with flame ionization detector using a column packed with a zeolite sample of interest [29].

Result and Discussion

(A) Mesoporous properties of monolithic silica

Various monolithic silicas were prepared from precipitated silica in powder-form (SiP) at different pressing pressures. Fig. 1A depicts the nitrogen adsorption isothermsof the precipitated silica samples. To avoid the interference of inter-particle voids, the monolithic silica was ground before the measurements of adsorption isotherms. The adsorption isotherms showed typical type IV with H3 hysteresis loop. The microporous and mesoporous surface areas of the ground monolithic silicas were about the same as that of powder silica SiP (Table 1). Even though, the ground monolithic silicas all possessed

higher pore volumes than the parent SiP. The average pore sizes of the ground monolithic silicas were in the vicinity of the parent SiP of 22.5 nm (Fig. 1B). The ground monolith silicas SiP140G and SiP280G show normal pore size distribution curves. Accordingly, pressurization at pressure of 140 and 280 kg/cm^2 generated uniform mesopores. SiP140G possessed the maximum pore size of 24.9 nm and pore volume of 1.0 cm3/g. In comparison, the SiP420G formed at pressure of 420 kg/cm2 generated irregular non-uniform mesopores having some mesopores large than SiP.

(B) Acid assisted crystallization of silica

The "boiling mode" and "steaming mode" were devised for conducting solid state crystallization of silica. With "boiling mode", crystallization of monolithic silica at pH of 5 by A protocol was studied at 180 ℃ for 12 h. Fig. 2 depicts the x-ray diffraction (XRD) patterns of the acid assisted conversion of monolithic silicas. All the ASiP samples except ASiP420 show high crystallinities with characteristic XRD peaks of the MFI phase with no impurity phase. It is usually difficult to form zeolite crystal from acidic solution by conventional hydrothermal process. The high crystallinities of ASiPz products suggest the application of A protocol for zeolite synthesis by the acid assisted conversion route. In comparison, the crystallinity of ASiP420 was relatively low, indicating a slow crystallization rate. By grinding SiP420 monolith into SiP420G powder, ASiP420G shows high crystallinity, indicating a significant acceleration of crystallization of SiP420G in powder form. Steam is crucial for the solid transformation process [30]. Mesopores act as steam reservoirs and meso-reactors for the conversion of amorphous silica into crystalline zeolite. Thus uniform mesopores is beneficial for solid state conversion process. As shown above, SiP420G had non-uniform mesopore size distribution. The pore size distribution of SiP420 could be even more non-uniform. Presumably, steam distribution in SiP420 was uneven with low diffusivity. The low crystallinity of ASiP420 could be attributed to the poor steam distribution inside the mesopores of silica. After being ground into powder form, SiP420G could have more mesoporous surface areas with improved steam distribution and reduced diffusion resistance in mesopores. Thus crystallization rate of ASiP420G has been accelerated.

Fig. 3 depicts the SEM images of the ASiPz products. In line with XRD results, the ASiP420 comprised large longitudinal rectangle crystals in 7 x 12 μm and aggregates of irregular silica nano-particles as an indication of the existence of amorphous materials. Interestingly, the ASiP420G has a uniform prism shape in the size of 3 x 10 μm. ASiP comprised prism crystals in 6 x 15 μm and small portion of amorphous materials. ASiP140 and ASiP280 show similar twin rectangle morphology. Their crystal sizes grown from monolithic silica were smaller than that grown from silica powder.

The nitrogen sorption isotherms of ASiPz products are shown in Fig. 4. SiP had low microporous surface area. Its adsorption isotherm crossed over those of ASiPz at P/P_0 in the range of 0.5 and 0.82, as a result of increasing micropore surface areas with decreasing pore volume as an indication of appearance of zeolite crystal phase. Notice that the mesoporous surface area of SiP stayed existing after crystallization. The crossover intersection P/P0 moved upward with increasing microporous surface area.

The monolithic silica product ASiP140 and ASiP280 and the ground monolith ASiP420G all show type I sorption isotherms, which are similar to a typical silicalite sample. ASiP420 show type IV isotherm with H3 hysteresis loop having a low micropore surface area and high mesopore volume. As a result, the microporous surface area was in the order of ASiP140 ~ ASiP280 ~ silicalite > ASiP420G > ASiP420 > SiP (Table 1), following the same order of crystallinity.

The pore size distribution is depicted in Fig. 4B. ASiP140 and ASiP280 show two major peaks centered at 2.3 and 3.9 nm. ASiP420G had less pore volume and small mesopore size of 3.9 nm. The ASiP140, ASiP280 and ASiP420G all are crystalline MFI. Their mesopores being smaller than 5 nm can be attributed to the inter-crystalline void of crystal aggregates. On the other hand, ASiP420 was a composite of MFI crystals and amorphous particle aggregates. The big mesopores in the range of 7 and 100 nm should be contributed from the inter-particle void of

amorphous silica particles. The micro/nano composite pore system could offer an improved diffusivity of ASiP420.

Adsorption properties of hexane isomers of the products were measured. As shown in Fig. 5, the typical commercial silicalite shows a duplex curve centered at 399 and 495 K. Although ASiP140, ASiP280 and silicalite showed similar nitrogen adsorption isotherms, their n-C6 TPD were different from each other. ASiP280 shows a duplex curve at desorption temperatures lower than that of silicalite. ASiP140 shows a singlet TPD centered at 435 K. On the other hand, due to low adsorption strength, mesoporous silica such as MCM-41 and amorphous material showed no TPD capacity. The different TPD indicates those MFI products have different micropore structures. As shown above, ASiP420 comprised MFI crystal and amorphous silica particle aggregates. Mesopore could facilitate the diffusion of hexane in micropores, leading to lower TPD temperatures [31]. Thus hexane TPD could be a sensitive tool to probethe subtle variations in the microporous structures of zeolites and used as a complementary tool for the BET isotherm. Compared to silicalite, ASiP140 and ASiP280 had about 150% n-hexane sorption capacities at lower desorption temperatures. These sorption properties indicate that ASiP140 and ASiP280 had widely open micropores, allowing hexane molecules for fast diffusion. Although ASiP420 comprised very large crystals, it had relatively low sorption temperature. It implies that the micropore channels were short, or fully accessible to external surface.

(C) Solid transformation protocols

Based on thermodynamic calculation, three crystallization protocols, either "boiling" or "steaming" mode, were devised for converting monolithic silica into MFI zeolite. With "boiling mode", the TPA-silica composite was impregnated with H_2SO_4 acidic solution or water of 0.2 ml for A or H protocol, respectively, then was placed in the bottom of an autoclave. The water usage was large enough to generate saturated steam in the autoclave, for example, 0.12 ml water for 25 ml vessel at 180 ℃. Therefore solid transformation was conducted in liquid phase. The final recipe of A and H protocol was 1 SiO_2 : 0.067 TPA : 2.36 H_2O. On the other hand, for "steaming mode" using D protocol, the TPA-silica composite was suspended on a frame seated in the autoclave above water level. The final recipe was 1 SiO_2 : 0.067 TPAOH. For 182 ml autoclave, 5 ml water was added to the bottom of the autoclave adequate for the generation of saturation steam inside the autoclave. Crystallization of TPA-silica composite using D protocol was a vapor phase process. Comparing to the conventional hydrothermal process, the SAC method produced very low aqueous solution waste.

The effect of crystallization protocol on the transformation of precipitated silica was studied. As shown in Figs. 6A and B, the ASiP or ASiP240 and HSiP or HSiP280, prepared with A or H protocol, all show strong XRD peak intensity of MFI crystalline phase. The zeolite crystals produced from silica powder, ASiP or HSiP, show stronger XRD peak intensity than the zeolite crystals grown from monolithic silica, ASiP280 and HSiP280, indicating a faster crystallization rate of powder silica than monolithic silica. The crystals grown from A and H protocols were in twin rectangle shape. The crystal prepared by the monolithic silica was in smaller crystal size than that prepared from powder silica SiP. HSiP280 showed uniform small crystal in the size of 700 nm, which was rarely reported for solid transformation process. In comparison, HSiP was in size of about 2 μm.

In contrast, the DSiP product produced from silica powder show weak XRD intensity (Fig. 6C) and a mixture morphology (SEM image Fig. 7c), suggested that DSiP was a composite of MFI crystal and silica particles. The DSiP280 showed strong XRD intensity of pure MFI phase and fine crystal morphology in SEM image without amorphous phase (Fig. 7f). The DSiP280 was multi-faced prisms in highly intergrowth in a large size of 2 x 6 m. Thus, in using D protocol, monolithic silica had faster crystallization rate than the powder silica. On the other hand, the crystallization rate of D protocol was slower than that of A or H protocol.

The sorption isotherms of various solid products crystallized from SiP using different protocols are shown in Fig. 8A. The ASiP and HSiP show type I adsorption isotherms with small hysteresis loops. Their microporous surface areas were higherthan 210 m^2g^{-1}. Their mesoporous

surface areas of around 105 m^2g^{-1} with pore size of around 3 nm and pore volume of 0.08 cm-3g-1 were all smaller than the original SiP. On the other hand, the DSiP showed type IV isotherm with H3 hysteresis loop at P/P_0 of 0.8. Comparing to ASiP and HSiP, DSiP had a lower micropore surface area and higher mesopore volume (Table 3). Its adsorption isotherm reflected the nature as a composite of partial crystalline MFI zeolite and the SiP280 silica particles.

Crystallization products from SiP280 show nitrogen adsorption isotherms with evident hysteresis loops at P/P_0 at 0.40, 0.45 and 0.89 for HSiP280, ASiP280 and DSiP280, respectively. The pore size increased with the order of H, A and D protocols. DSiP280 had a significant high pore size of 4.8 nm with a pore volume of 0.13 cm^3g^{-1}.

Therefore, the solid state crystallization is a versatile process for tuning the morphology and properties of the zeolite crystal products. Crystallization of amorphous silica into crystalline zeolite involves complicated crystallization mechanism. It is a silica rearrangement reaction comprising silica decomposition and condensation of the silanol groups with formation of T-O-T network. Arnold et al. demonstrated that DGC process starts with excessive chemical bonds breakage into defect SiOH groups, followed by the condensation of terminal bonds with decreasing OH concentration of silanol groups and Q^1, Q^2 and Q^3 silicon species [32]. During the whole DGC process, SDA cation is stabilized by dry gel and remained unchanged [32, 33].

Since highly porous zeolites have lower framework densities and higher molar volumes than amorphous silica [34], amorphous silica framework expands during the solid transformation. Presumably, silica crystallizes on the wall of pores or external surface where water is accessible. With increasing reaction time, increasing condensation of silanol groups to form more crystalline framework with formation of water. Along with zeolite growth, as a result of volume expansion, the mesopores of the silica precursors collapse or shrunk with reduced pore volume and mesopore size. There were no porogen generating agent, such as carbon used for templated synthesis [27], in the proposed protocol for protecting the amorphous walls of monolithic silica beyond collapse during crystallization. Zhou et al. reported that drying temperature can significantly affect the extent of condensation of the -Si–O network in themesoporous framework and thus the mesoporosity of zeolite products [28]. Jung et al. reported that there is a memory effect of morphology of dry gel on zeolite crystal depending on the amount of TPAOH and the crystallization condition [35]. Therefore, process conditions could have important effects.

With “steaming” mode, the solid state crystallization of the stabilized TPA-silica composite occurs in the region of mesopores or external surface where steam is accessible. Comparing to powder silica, the monolithic silica had larger pore volume (Table 1) and closer contact between silica particles. The higher crystallinity of DSiP280 than DSiP could be attributed to the higher water content accumulated inside mesopores of monolithic silica. Monolithic silica has an optimum pressurization pressure for mesoporosity generation. Maximum pressure is limited by the formation of irregular mesoporous structure to get away from diffusion resistance in mesopore.

On the other hand, silica particles are in close contact each other in the solid state crystallization. Therefore, zeolite crystal nuclei tend to intergrowth into large crystal size. The MFI crystals grown from powder silica and monolithic silica were about the same size in 2 x 6 m rectangle (Fig. 7f).

With “boiling” mode, the water content in the starting gel was oversaturated. Notice that water was a by-product generated from the condensation of silanol. Therefore, during the whole transformation process, silica crystallization was conducted in liquid phase. The “boiling” mode was similar to the conventional hydrothermal process. Water is very essential for facilitating the crystallization of silica and zeolite formation [30]. In the absence of water in the bottom of autoclave, there was no crystallization. Nevertheless, Matsukata et al. proposed that by maintaining saturated vapor pressure in an autoclave, water usage should be minimized to prevent from excessive water condensation in the gel and degradation of SDA in the aqueous phase [33].

The A and H protocols involved silica dissolution and

polymerization in liquid phase, and probably dissolution of TPA. As shown above, the A and H protocols had faster silica crystallization rate but less mesoporosity generation than D protocol. The MFI crystal size grown from monolithic silica was smaller than that grown from silica powder (Figs. 3, 7). Their differences might be attributed to the water effect. The liquid phase used in the A and H protocol contains condensed water which is detrimental to the stability of TPA-silica composite.

As demonstrated above, the solid crystallization method is simple, easy and environmental sound and more importantly versatile for preparing MFI crystals with variety of morphology in the crystal size ranging from nm to μm and porous structures. Comparing to protocol A and H, protocol D is more effective in generating mesopores from monolithic silica.

Conclusion

A facile and versatile solid crystallization method is developed for converting pre-formed monolithic silica into mesoporous MFI zeolite with variety of crystal morphology in the crystal size ranging from 700 nm to 10 μm and meso/mico porous structures. Among the devised protocols, protocol D (steaming mode) is more effective than protocol A and H (boiling mode) for generating mesoporosity in MFI zeolite, while the latter has faster crystallization rate than the former. Whereas in steaming mode monolithic silica has faster crystallization rate than the powder silica, in boiling mode crystallization of powder silica is faster than monolithic silica. Their differences might be attributed to the operating phase and water effect.

During solid state crystallization, the mesoporous surface area of the parent monolithic silica stays unchanged. With increasing crystallinity, micropore surface areas increase with decreasing pore volume. Optimum hierarchical porosity can beoptimized by selecting appropriate crystallization protocol and conditions. The micro/meso porous MFI crystals show enhanced hexane sorption capacity, about 150% sorption capacities of normal silicalite, at lower desorption temperatures.

Acknowledgements

We wish to thank Dr. Hon-Pin Lin for SEM measurements. This study was financially supported by National Science Council, Republic of China under grant NSC 98-2113-M-390-003-MY3.

Reference

[1] T.O. Drews, M. Tsapatsis, Curr. Opin. Colloid Interface Sci., 10 (2005) 233.

[2] R. Srivastava, M. Choi, R. Ryoo, Chem. Commun., (2006) 4489.

[3] W.C. Li, A.H. Lu, R. Palkovits, W. Schmidt, B. Spliethoff, F. Schűth, J. Am.. Chem. Soc., 127 (2005) 12595.

[4] M.B.Yue, L.B. Sun, T.T Zhuang, X. Dong, Y. Chun, J.H. Zhu, J. Mater. Chem., 18 (2008) 2044.

[5] S.T. Tsai, C.H. Chen, T.C. Tsai, Green Chem., 11 (2009) 1349.

[6] C. Madsen, C.J.H. Jacobsen, Chem. Commun., (1999) 673.

[7] L. Tosheva, V.P. Valtchev, Chem. Mater., 17 (2005) 2494.

[8] J. Pérez-Ramírez, C.H. Christensen, K. Egeblad, C.H. Christensen, J.C. Groen, Chem. Soc. Rev., 37 (2008) 2530.

[9] Y. Tao, H. Kanoh, L. Abrams, K. Kaneko, Chem. Rev., 106 (2006) 896.

[10] J. Čejka, S. Mintova, Catal. Rev. Sci. Eng., 49(4) (2007) 457.

[11] A. van Miltenburg, J. Pawlesa, A. M. Bouzga, N. Žilková, J. Čejka, M. Stöcker, Top. Catal., 52 (2009) 1190.

[12] J. Lee, J. Kim, T. Hyeon, Adv. Mater., 18 (2006) 2073.

[13] K. Egeblad, C.H. Christensen, M. Kustova, C.H. Christensen, Chem. Mater., 20 (2008) 946.

[14] Y. Wan, D. Zhao, Chem. Rev., 107 (2007) 2821.

[15] Z.L. Hua, J. Zhou, J.L. Shi, Chem. Commun., 47 (2011) 10536.

[16] X. S. Zhao, F. Su, Q.F. Yan, W. Guo, X.Y. Bao, L. Lv, Z. Zhou, J. Mater. Chem., 16 (2006) 637.

[17] T. Yokoi, T. Tatsumi, Jpn. Pet. Inst., 50 (2007) 299.

[18] A. Thomas, F. Goettmann, M. Antonietti**,** Chem. Mater., 20 (2008) 738.

[19] X. Meng, F. Nawaz, F.S. Xiao, Nano Today, 4 (2009) 292.

[20] J. Zhou, Z. Hua, J.J. Zhao, Z. Gao, S.Z. Zeng, J.L. Shi,

J. Mater. Chem., 20 (2010) 6764.
[21] F. Schüth, Angew. Chem., Int. Ed., 42 (2003) 3604.
[22] C.J.H. Jacobsen, C. Madsen, J. Houzvicka, I. Schmidt, A. Carlsson, J. Am. Chem. Soc., 122 (2000) 7116.
[23] Y. Tong, T. Zhao, F. Li, Y. Wang, Chem. Mater., 18 (2006) 4218.
[24] M.K. Choi, H.S. Cho, R. Srivastava, C. Venkatesan, D.-H. Chi, R. Ryoo, Nat. Mater., 5 (2006) 718.
[25] H. Zhu, Z. Liu, Y. Wang, D. Kong, X. Yuan, Z. Xie, Chem. Mater., 20 (2008) 1134.
[26] J. Zhao, J. Zhou, Y. Chen, Q. He, M. Ruan, L. Guo, J. Shi, H. Chen, J. Mater. Chem., 19 (2009) 7614.
[27] Y. Tong, T. Zhao, F. Li, Y. Wang, Chem. Mater., 18, (2006) 4218.
[28] J. Zhou, Z. Hua, J.J. Zhao, Z. Gao, S.Z. Zeng and J.L. Shi., J. Mater. Chem., 20 (2010) 6764.
[29] P.Y. Chao, Y.Y. Chuang, G.H. Ho, S.H. Chuang, T.C. Tsai, C.Y. Lee, S.T. Tsai, J.F. Huang, J. Chem. Edu., 85(11) (2008) 1558.
[30] T. Tatsumi, Q. Xia, N. Jappar, Chem. Lett., (1997) 677..
[31] S. van Donk, A. Broersma, O.L.J. Gijzeman, J.A. van Bokhoven, J.H. Bitter and K. P. de Jong, J. Catal., 204 (2001) 272..
[32] A. Arnold, S. Steuernagel, M. Hunger, J. Weitkamp, Microporous. Mesoporous Mater., 62 (2003) 97.
[33] M. Matsukata, M. Ogura, T. Osaki, P. R. H. P. Rao, M. Nomura, E. Kikuchi, Top. Catal., 9 (1999) 77.
[34] A. Navrotsky, O. Trofymluk, A.A. Levchenko, Chem. Rev. 109 (2009) 3885.
[35] K.T. Jung, Y.G. Shul, Microporous. Mesoporous. Mater. 21 (1998) 281.

	S_{BET} /m^2g^{-1}	S_{meso}/m^2g^{-1}	S_{micro}/m^2g^{-1}	V_{meso}/cm^3g^{-1}	D_{pore}/nm
Silica powder					
SiP	154.7	131.9	22.8	0.60	22.5
Monolithic silica					
SiP420G	159.4	161.9	25.7	0.80	20.2
SiP280G	158.9	135.8	23.1	0.81	20.5
SiP140G	156.2	131.9	24.3	1.00	24.9
Acid assisted crystallization of silica (A protocol)					
ASiP	339.6	105.1	234.5	0.09	3.4
ASiP140	334.1	121.3	212.8	0.09	3.1
ASiP280	332.1	109.4	222.8	0.08	3.0
ASiP420	183.7	104.7	78.9	0.19	10.0
ASiP420G	336.8	195.4	141.4	0.06	2.7

Table 1 Textural properties of precipitated silica powder, monolithic silica and Acid assisted crystallization of silica using A protocol

	n-C6		3-MP	
	W_{des}	T_{des}	W_{des}	T_{des}
Silicalite	7.2 wt%	399, 495 K	-	-
ASiP140	10.8 wt%	435 K	8.1 wt%	423 K
ASiP280	11.2 wt%	392 K , 448 K	8.7 wt%	435 K
ASiP420	3.9 wt%	396 K	1.6 wt%	360 K

Table 2 Hexane temperature programmed desorption of acid assisted crystallization of silica with A protocol

	S_{BET}/m^2g^{-1}	S_{meso}/m^2g^{-1}	S_{micro}/m^2g^{-1}	V_{meso}/cm^3g^{-1}	D_{pore}/nm
HSiP	318.9	106.7	212.2	0.08	2.9
ASiP	339.6	105.1	234.5	0.09	3.4
DSiP	185.2	111.7	73.5	0.20	9.5
ASiP280	332.1	109.4	222.8	0.08	3.0
HSiP280	368.6	99.9	268.6	0.07	2.9
DSiP280	288.5	114.6	173.8	0.13	4.8

Table 3 Textural properties of steam assisted conversion of silica powder and monolithic silica using different protocols

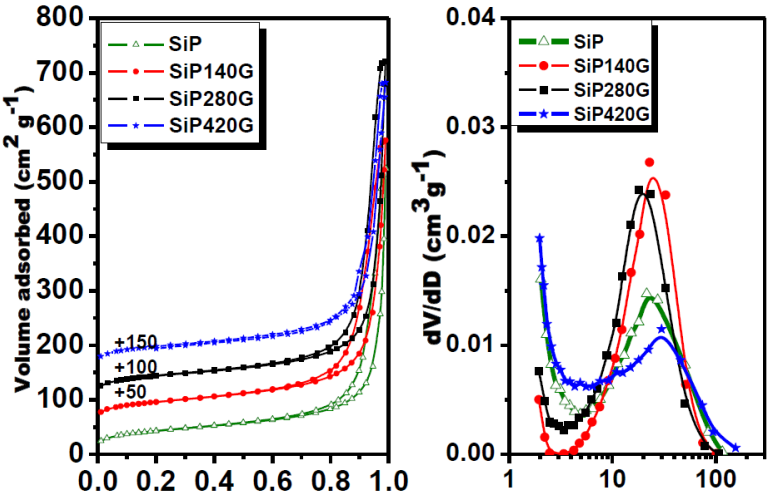

Fig. 1 Nitrogen adsorption isotherms (offset by 50 m^2/g) (A); and pore size distribution (B) of precipitated silica in powder and ground monolith form

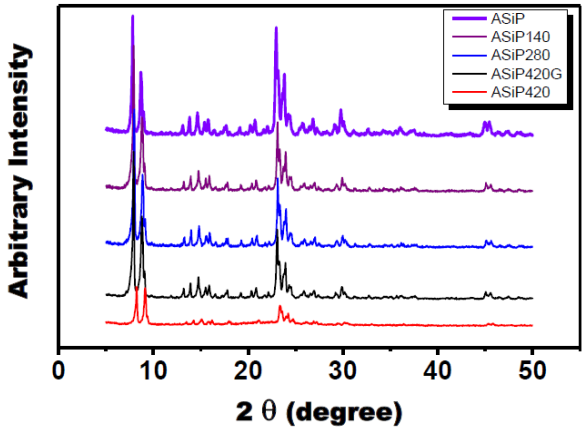

Fig. 2 X-ray diffraction patterns of steam assisted conversion products

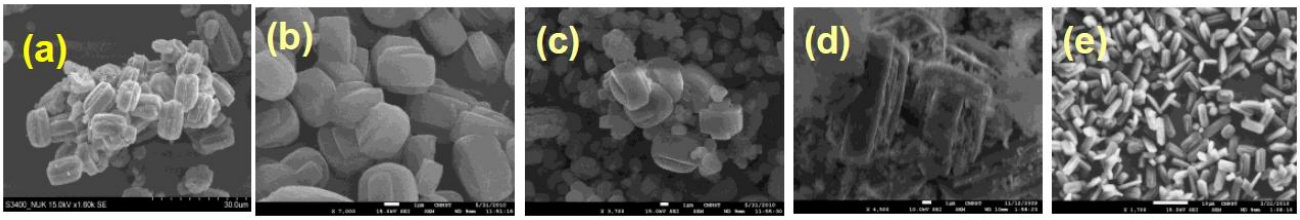

Fig. 3 SEM images of steam assisted conversion products prepared from (a) powder silica (ASiP) and monolithic silica (b) ASiP140; (c) ASiP280; (d) ASiP420; (e)ASiP420G.

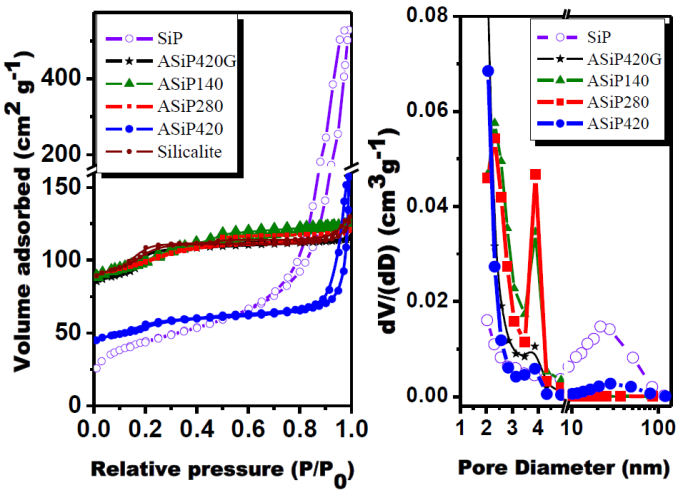

Fig. 4 Nitrogen adsorption isotherms (A) and pore size distribution (B) of precipitated silica in powder and monolith form

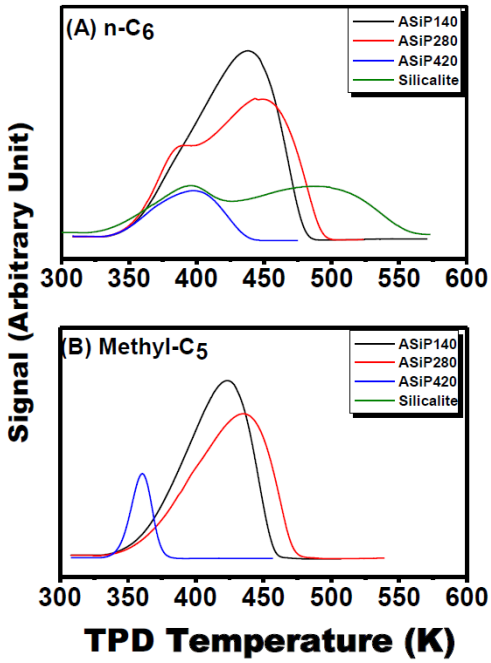

Fig. 5 Temperature programmed desorption of (A) n-hexane; (B) methy-pentane of acid assisted conversion of silica

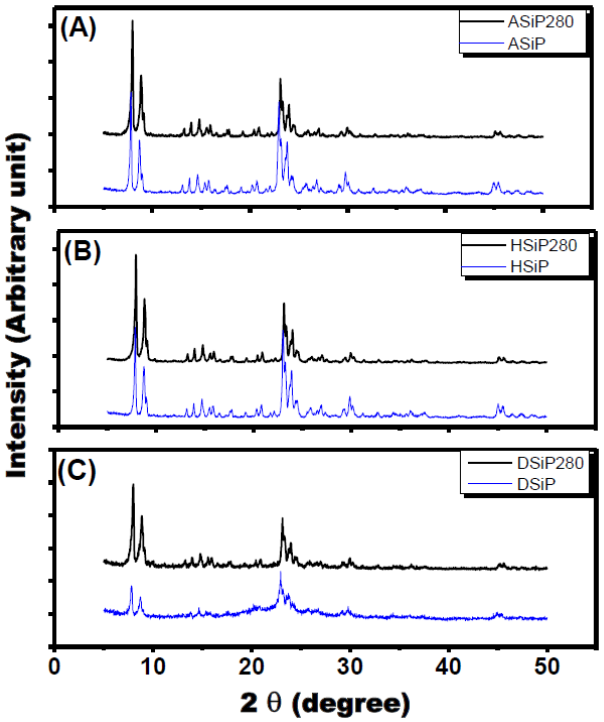

Fig. 6 X-ray diffraction patterns of steam assisted conversion of silica power and monolithic silica pre-formed at 280 psig using (A) A; (B) H; and (C) D protocol.

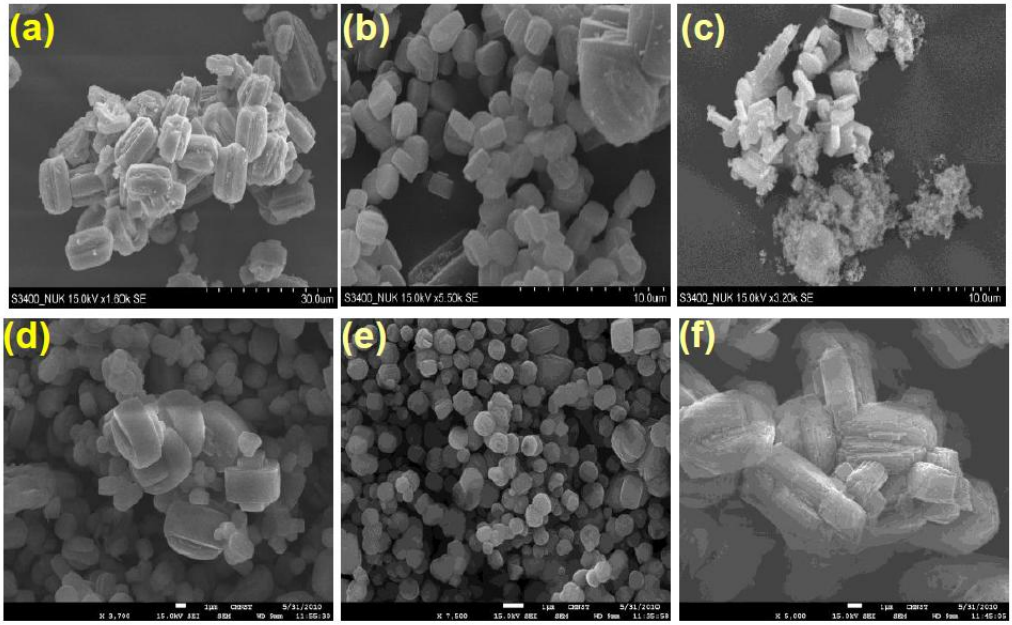

Fig. 7 SEM images of steam assisted conversion products (a) ASiP; (b) HSiP; (c) DSiP; (d) ASiP280; (e) HSiP280; (f) DSiP280.

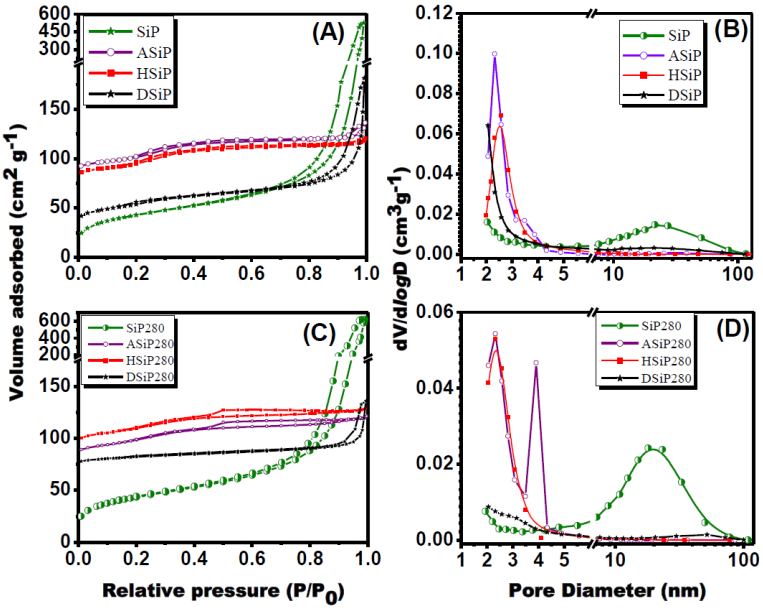

Fig. 8 Nitrogen sorption isotherm (A) and pore size distribution (B) of solid transformation products of SiP; nitrogen sorption isotherm (C) and pore size distribution (D) of monolithic silica SiP280 by A, H and D protocols